# Scaling of the critical temperature with the Fermi temperature in diborides

A. Bianconi,* S. Agrestini, D. Di Castro, G. Campi, G. Zangari, and N. L. Saini
*Dipartimento di Fisica and Istituto Nazionale di Fisica della Materia, Università di Roma "La Sapienza," P. le Aldo Moro 2, 00185 Roma, Italy*

A. Saccone, S. De Negri, and M. Giovannini
*Dipartimento di Chimica e Chimica Industriale, Università di Genova, Via Dodecaneso 31, 16146 Genova, Italy*

G. Profeta and A. Continenza
*Istituto Nazionale di Fisica della Materia and Dipartimento di Fisica, Università dell'Aquila, L'Aquila, Italy*

G. Satta and S. Massidda
*Istituto Nazionale di Fisica della Materia and Dipartimento di Fisica dell'Università di Cagliari, Cagliari, Italy*

A. Cassetta and A. Pifferi
*Istituto di Strutturistica chimica del CNR, Area Ricerca di Roma, Montelibretti 00016 Monterotondo Stazione, Italy*

M. Colapietro
*Dipartimento di Chimica, Università di Roma "La Sapienza," P. le Aldo Moro 2, 00185 Roma, Italy*
(Received 22 January 2002; published 23 April 2002)

The experimental determination of the scaling of the superconducting critical temperature ($T_c$) vs the Fermi temperature ($T_f$) of the holes in the boron $\sigma$ subband is presented. The Fermi level has been tuned near the "shape resonance," i.e., the two- to three-dimensional crossover of the Fermi surface of the boron $\sigma$ subband by changing the Al/Mg content in $Al_{1-x}Mg_xB_2$. The product $k_f\xi_0$ of the Fermi wave vector ($k_f$) times the superconducting Pippard coherence length ($\xi_0$), that is a measure of the pairing strength, remains constant, $k_f\xi_0=90$ for $x>0.66$. This high-$T_c$ phase occurs in the boron superlattice under a tensile microstrain in the range $3\%<\varepsilon<6\%$.

DOI: 10.1103/PhysRevB.65.174515 PACS number(s): 74.70.Ad, 74.25.Dw, 74.25.Jb, 74.62.−c

The recent discovery of a high-$T_c$ phase in $MgB_2$ (Ref. 1) and $C_{60}$, intercalated with $CHBr_3$,[2] showed that the high-$T_c$ phase occurs in metallic heterostructures at the atomic limit,[3] where a superlattice is made of metallic units (boron layers or $C_{60}$ buckyballs) intercalated by a different material (Mg layers or $CHBr_3$ molecules). According to Ref. 3, the process for $T_c$ amplification in these systems requires tuning the Fermi level at a "shape resonance" of the superlattice where the Fermi velocity in the direction of the superlattice modulation goes to zero and the Fermi surface topology shows a dimensional crossover.[3] $MgB_2$ is a diboride where the Fermi level $E_F$ is below the top of the $\sigma$ subband of the boron superlattice at $E_A$.[4] $AlB_2$ is the prototype compound for this structure type, where conversely, the Fermi level is at $E_F > E_A$ as in most of diborides.[5] The synthesis of $Mg_xAl_{1-x}B_2$ series was first reported by Vekshina *et al.*[6] The drop of $T_c$ by decreasing the Mg content[7–12] was associated with the filling of the $\sigma$ subband of the sublattice of boron layers.[9,13] The data of Ref. 7 were interpreted by An and Pickett[4] using a rigid band of the $MgB_2$ band structure (where, by changing the $Al^{3+}/Mg^{2+}$ ratio, only $E_F$ shifts). However, the rigid-band model fails to describe the physics of an $Al_{1-x}Mg_xB_2$ system, since the substitution of large $Mg^{2+}$ ions in the hexagonal $Al^{3+}$ lattice induces not only a change of the number of valence electrons but also an expansion of both the *a* and *c* axes of the boron superlattice, with the associated variation of the band dispersion and the shift of the top of the $\sigma$ subband, as shown by recent calculations using a non-rigid-band model.[5,13] In the $AlB_2$ structure there is a good lattice matching between the graphitelike boron lattice and the hexagonal hcp lattice of Al with a microstrain $\varepsilon=(a-a_0)/a_0$, where $a_0=c/1.075$ is the equilibrium distance in a perfect $AlB_2$ lattice.

In this work we study the onset of the high-$T_c$ phase going from $AlB_2$ to $MgB_2$ by a synthesis of solid solutions $Al_{1-x}Mg_xB_2$, with a variable Mg content, and the results are compared with a full band-structure calculation. The present results provide a solid experimental base for the understanding of the onset of the high-$T_c$ phase coming from the low-$T_c$ metallic phase induced by changing both the charge density and the microstrain of the boron sublattice.

*First*, we synthesized high-purity samples, avoiding the use of quartz tube, that were used in Ref. 7, for preparation of the diborides, since the Mg gas at high temperature reacts with quartz and induces MgO impurity phases in the final compound. *Second*, we measured a large number of samples in order to identify with high accuracy the point of the sharp drop of $T_c$ expected at the two-dimensional 2D-3D crossover in the Fermi surface of the $\sigma$ subband. *Third*, we characterized the Al/Mg lattice disorder of our samples with high resolution x-ray diffraction using synchrotron radiation. *Fourth*, we measured the lattice parameters at each value of *x*. *Finally*, we carried out an accurate band structure calculation for each Mg content *x* with its lattice parameters in order

 

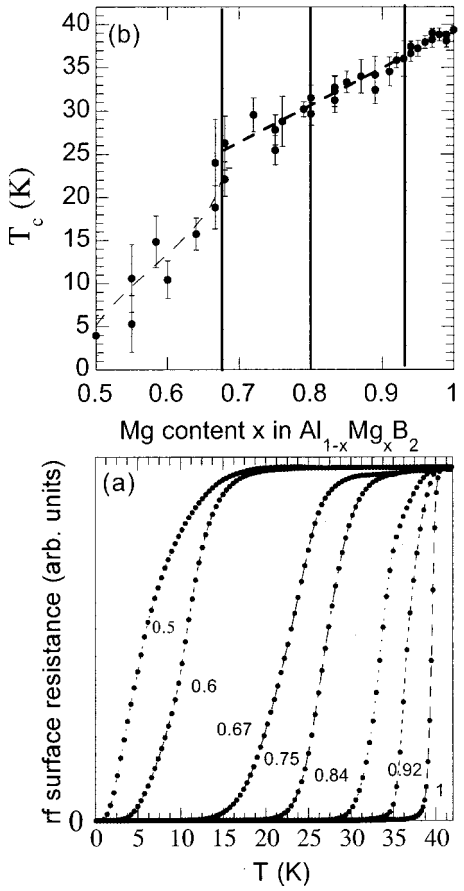


FIG. 1. (a) The radio-frequency complex conductivity probed by the ratio $f_0(T)^2/f(T)^2$, where $f_0(T)$ and $f(T)$ are the resonance frequencies of the probing LC circuit measured without and with the sample, respectively. The ratio $f_0(T)^2/f(T)^2$ is measured for different $Al_{1-x}Mg_xB_2$ samples for different values of $x$. (b) The critical temperature $T_c$ as a function of Mg content $x$ given by the peak of the derivative of the $f_0(T)^2/f(T)^2$ curves.

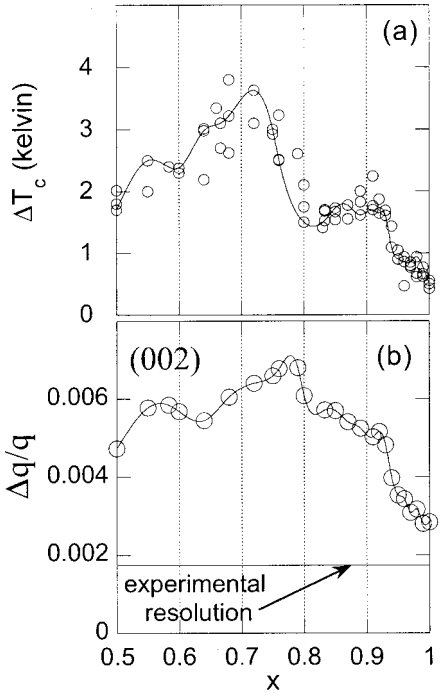


FIG. 2. (a) The width of the superconducting transition $\Delta T_c$ of $Al_{1-x}Mg_xB_2$ as a function of $x$, (b) The relative width $\Delta q/q$ (where $q=2\pi/\lambda$ is the momentum transfer) of the (002) diffraction line at low temperature $T=100$ K. A collimated synchrotron radiation beam of photon wavelength $\lambda=100$ pm has been used. The experimental resolution is $\Delta q/q=1.7\times10^{-3}$ determined by using a silicon single crystal.

to calculate the position of the Fermi level relative to the top of the $\sigma$ subband and the 2D-3D crossover, overcoming the limitations of the rigid-band approximation.

We report the sharp drop of $T_c$ at $x<0.66$, and show that it is associated with the 2D-3D crossover in the $\sigma$ subband calculated by full band-structure calculations. High-resolution x-ray-diffraction (XRD) shows a order-disorder transition at $x=0.93$ induced by the Al/Mg lattice disorder for $x<0.93$. For $x<0.93$ the structural disorder, due to the formation of domains with different Al/Mg ratios, is correlated with the broadening of the superconducting transition width, indicating the formation of mesoscopic domains with different $T_c$. However the lattice disorder, for $0.5<x<0.93$, induces only a minor effect on $T_c$. Finally we show that superconducting diborides $Al_{1-x}Mg_xB_2$ have a constant intermediate coupling strength (between cuprates and low-$T_c$ superconductors), and that $T_c$ is linear with the Fermi temperature in the range $0.66<x<1$.

High-quality $Al_{1-x}Mg_xB_2$ samples were synthesized by a direct reaction of the elemental magnesium, aluminum (rod, 99.9% mass, nominal purity) and boron (99.5% pure $<60$ mesh powder). The elements in a stoichiometry ratio were enclosed in tantalum crucibles, sealed by arc welding under an argon atmosphere. The Ta crucibles were then sealed in a heavy iron cylinder and heated for 1 h at 800 °C and 2 h at 950 °C. We have avoided the use of a quartz tube for the preparation of the diborides. The phase purity was checked by x-ray diffraction measured using high-intensity synchrotron light, emitted by a wiggler source, at the third generation Elettra storage ring, operated at 2 Gev and 170 mA. The diffraction patterns were recorded on the XRD beam line

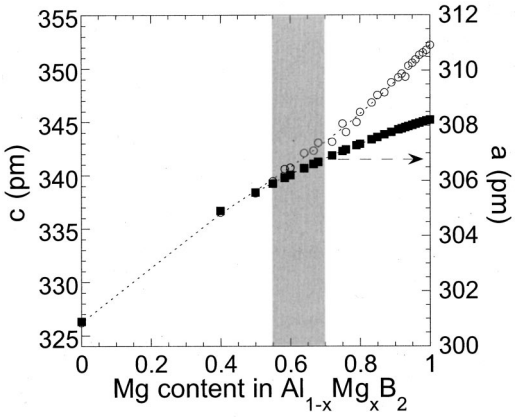


FIG. 3. The variation of the $a(x)$ and $c(x)$ axes (1 pm $=0.001$ nm) as a function of Mg doping $x$ in $Al_{1-x}Mg_xB_2$ samples measured by high-resolution x-ray diffraction.

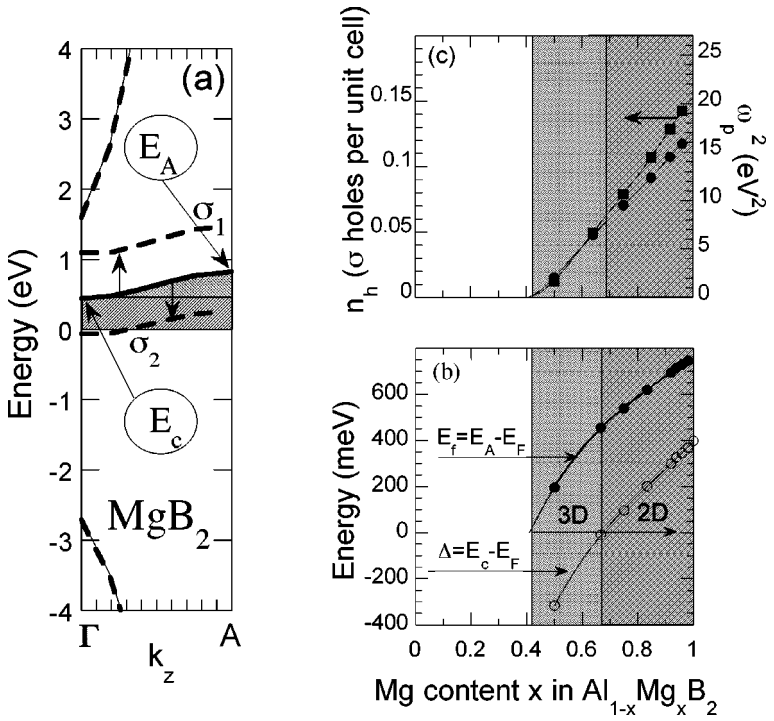


FIG. 4. (a) The band structure of $MgB_2$ in the $\Gamma$-$A$ direction of the Brillouin zone for the direction of the wave vector perpendicular to the boron monolayers. The top of the $\sigma$ subband, made of $2p_{x,y}$ boron orbitals, occurs at the energy $E_A$ at the $A$ point. The hopping between the boron monolayers gives the dispersion of the holelike band from $A$ to $\Gamma$ points at the energy $E_c$. A quantum critical point is at energy $E_c$ where a dimensional transition occurs from a 2D-like $\sigma$ Fermi surface at $E_F<E_c$ to a 3D-like one in the range $E_c<E_F<E_A$. The $E_{2g}$ Raman-active phonon mode induces a large splitting of the two degenerate $\sigma$ subbands. The 800-meV energy splitting of $\sigma_1$ and $\sigma_2$ subbands for a 5-pm frozen lattice distortion of $E_{2g}$ type is shown by dashed curves. (b) The shift of the chemical potential $E_F$ relative to the top of the $\sigma$ band at $E_A$ that gives the Fermi energy for the holes in the $\sigma$ band $E_f(x)=E_A(x)-E_F(x)$, and $\Delta(x)=E_c(x)-E_F(x)$, where $E_c$ is the QCP of the boron $\sigma$ $2p_{x,y}$ band, where a 2D to 3D transition occurs. (c) The number of holes per unit cell $n_h$ in the $\sigma$ subband and the square of plasma frequency ${\omega_p}^2$ proportional to $n_h/m^*$ as a function of Mg doping $x$.

using synchrotron light monochromatized by a double-crystal Si(111) monochromator, and focused on the sample by a Pt-coated silicon mirror. A CCD detector of 165-mm diameter, with $2048\times2048$ pixels per frame, with a pixel size of 79 $\mu$m, from Mar research, was used to record the diffraction patterns. This approach allowed us to determine the structural parameters with a high precision, reaching a momentum resolution of $\Delta q/q=1.7\times10^{-3}$ as measured by using a silicon crystal.

The superconducting properties were investigated by the temperature dependence of the complex conductivity using the single-coil inductance method.[14] The temperature-dependent radio-frequency complex conductivity for several Mg contents is shown in Fig. 1(a). The critical temperature for superconductivity in $Al_{1-x}Mg_xB_2$ shows various regimes as a function of Mg content Fig. 1(b). In the high-$T_c$ regime ($39.5>T_c>24$ K) the critical temperature shows a nearly linear decrease for decreasing $x$ in the range $1>x>0.66$ and, at $x=0.66$, it shows a sharp decrease toward the low-$T_c$ superconductivity regime $15>T_c>5$ K. Minor jumps of about 2 K in the curve $T_c(x)$ are observed at $x=0.93$ and 0.8. Figure 2(a) shows that the width of the transition $\Delta T_c$ is very narrow (0.4–1 K) for $x>0.93$. In the range $x<0.93$ the width of the transition becomes very large (2–4 K), and it is assigned to a glassy phase made of superconducting domains of a few times the superconducting coherence length with different critical temperatures. Using the high resolution of our synchrotron radiation diffraction system (that is several times better than the standard laboratory XRD system used in Ref. 7), we investigated the lattice disorder in the distribution of the spacing between the boron monolayers. Figure 2(b) shows the evolution of the width of the (002) reflections, measured at 100 K as a function of Mg doping. We observe a sharp onset of disorder for $x<0.93$, due to the formations of domains of nonuniform distribution of Al/Mg ions, that is well correlated with the broadening of the superconducting transition temperature.

The lattice parameters $a(x)$ and $c(x)$, determined by standard least-squares refinement of the diffraction patterns, are shown in Fig. 3. Both $a(x)$ and $c(x)$ increase under an expansion driven by the substitution of Mg ions with larger atomic radius at the Al sites. However, the rates of expansion of the lattice of boron monolayers (the $a$ axis) and the expansion of the spacing between the boron monolayers (the $c$ axis) are different. The resulting anisotropic volume expansion is indicated by the different behaviors of curves $a(x)$ and $c(x)$. In Fig. 3 we observe two main different regimes with different elastic constants separated by an intermediate region $0.55<x<0.7$ as a function of Mg content.

In the $Al_{1-x}Mg_xB_2$ system, the electron density, as well as the lattice parameters, change with the Mg doping. There-

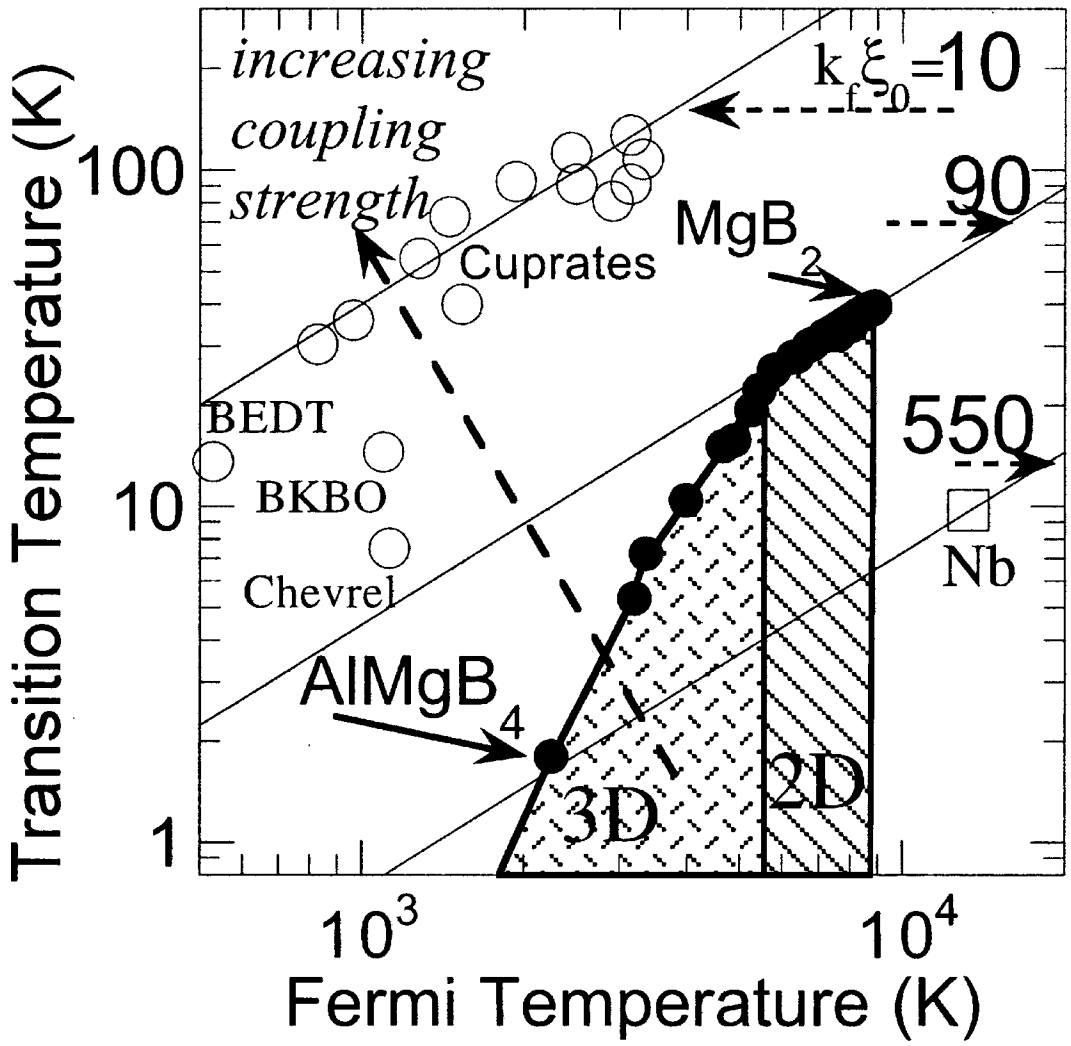


FIG. 5. The plot of the critical temperature $T_c$ in $Al_{1-x}Mg_xB_2$ vs the Fermi temperature $T_f$ compared with other superconductors Nb, and 1D organics, cuprates. The curve $T_c(T_f)$ scales as $T_c=(0.4/k_f\xi_0)T_f$, with a constant $k_f\xi_0=90$ for $0.66<x<1$. At $x=0.5$ the superconducting phase is in the low-$T_c$ regime, with $k_f\xi_0=550$ as in Nb. A sharp amplification of $T_c$ occurs in the dashed 3D-like region. The scaling law changes where the Fermi level is tuned at the quantum critical point for the transition from a 3D→2D topology of the Fermi surface.

fore, full band-structure calculations were performed using the ''all-electron'' full potential linearized augmented plane waves method,[5] in the local-density approximation to the density-functional theory. We used a plane-wave cutoff $k_{\max}=4.1$ a.u. and an accurate angular momentum expansion inside atomic spheres.

The Brillouin-zone sampling was performed using the linear tetrahedra method with 120-K points in the irreducible Brillouin zone. A spline fitting of eigenvalues was used to accurately check the position of the Fermi level. We have calculated the band edge positions in the two following ways: (i) by use of an ordered supercell, which results in a reasonably small unit cell for $x=0.25$, $\frac{1}{3}$, and 0.5; and (ii) by the simulation of a random Al/Mg distribution, substituting Mg with a virtual cation having nuclear charge $Z=13-x$. These two independent calculations, sharing the experimental lattice parameters, yield almost identical results (within about 15 meV), which shows that Al ordering effects are not important in this context.

In Fig. 4(a) we show the band structure of $MgB_2$ in the $\Gamma-A$ direction, and in Fig. 4(b) we show the variation of the Fermi energy for the holes in the $\sigma$ band: $E_f=E_A(x)-E_F(x)$, determined by the energy difference between the top of the 2D boron $\sigma(2p_{x,y})$ subband and the chemical potential $E_F(x)$. We also report the energy separation $\Delta=E_c(x)-E_F(x)$ between $E_F$ and the critical point $E_c$ at the $\Gamma$ point for the transition of the Fermi surface of the $\sigma$ subband between 3D and 2D-like behaviors. The critical temperature increases for $E_f>0$, where the number of holes in the $\sigma$ subband ($N_h$) is nonzero. The number of holes per unit cell $n_h$, and the plasma frequency for the holes, are plotted in Fig. 4(b). The Fermi temperature of the holes in the $\sigma$ subband, $T_f(x)=\{E_A(x)-E_F(x)\}/K_B$, is zero at $x=0.41$, and the number of $\sigma$ holes per unit cell increases from $n_h=0$ to 0.16 at $x=1$. The superconductivity appears for $T_f>0$, and increases with $T_f(x)$. The variation of the topology of the $\sigma$ Fermi surface from a 3D-like phase to a 2D-like phase occurs at $x=0.66$, where we observe a clear change in the slope of the $T_c(x)$ curve. The relative position of the

Fermi level from the top of the $\sigma$ subband, going from $AlMgB_4$ to $MgB_2$, is tuned over a range of 750 meV. This is the same energy range spanned, in $MgB_2$, by the splitting of the top of the $\sigma$ band into two subbands $\sigma_1$ and $\sigma_2$, due to the anharmonic $E_{2g}$ mode, with an amplitude of the in-plane lattice parameter of 5 pm, as shown in Fig. 4, in agreement with Yildirim *et al.*[15]

It is well known that for electronic pairing mechanisms[16] the superconducting critical temperature scales as the Fermi temperature. For cuprates and organic superconductors it was established that $T_c$ scales as $n_s/m^*$,[17] that is equivalent to $T_c=(0.4/k_f\xi_0)T_f$, with $k_f\xi_0=10$.[18] We plot the critical temperature $T_c$ as a function of the Fermi temperature in Fig. 5. From this phase diagram it is clear that, for $0.66<x<1$, the curve $T_c(T_f)$ follows a universal line where $T_c$ scales as $T_f$ with a constant $k_f\xi_0=90$. The value of $k_f\xi_0=90$ is a measure of the coupling strength for the pairing mechanism, that remains constant in this regime at an intermediate value between $k_f\xi_0=10$ for cuprates and 1D organics and $k_f\xi_0=550$ for a conventional low-temperature superconductor as Nb. In this range the Fermi surface is 2D-like. In the range $0.5<x<0.66$, where the Fermi surface is 3D-like due to electron hopping between boron layers, the coupling strength rapidly changes from the weak-coupling regime $k_f\xi_0=550$ in $AlMgB_4$, where the Fermi level is tuned near the top of the $\sigma$ subband at the $A$ point, to the intermediate coupling regime $k_f\xi_0=90$, by tuning the Fermi level at the critical point at the $\Gamma$ point where $G-2k_F=2\pi/c$, i.e., the Fermi wavelength of the holes is of the order of the spacing $c$ between the boron layers.[3]

In summary, we have studied the origin of $T_c$ amplification in $Al_{1-x}Mg_xB_2$ from 5 K in $AlMgB_4$ to 39 K in $MgB_2$. The disorder due to random Mg/Al distribution in the hexagonal monolayers intercalated between graphitelike boron monolayers, revealed by high-resolution diffraction measurements, induces a broadening of the superconducting transition, but has only a minor effect on the value of $T_c$. The sharp amplification of $T_c$ occurs where the chemical potential reaches the 2D-3D Fermi-surface crossover at $x=0.66$. We have identified two scaling regimes—the first for $x<0.66$ (where the topology of the Fermi surface of the $\sigma$ band is 3D-like), and the second for $x>0.66$ (where the topology of the Fermi surface is 2D-like)—with a constant $k_f\xi_0=90$. The results of the present work show a linear scaling of $T_c$ versus $T_f$ in $Al_{1-x}Mg_xB_2$ for $1>x>0.66$, pointing toward a vibronic pairing mechanism in diborides like in cuprates.[19]

This work was supported by ''progetto cofinanziamento ''Leghe e composti intermetallici: stabilità termodinamica, proprietà fisiche e reattività'' of MIUR, Istituto Nazionale di Fisica della Materia'' (INFM), and by ''Progetto 5% Superconduttività of Consiglio Nazionale delle Ricerche'' (CNR).

*Author to whom correspondence should be addressed.
Email address: bianconi@superstripes.com
For further information see http://www.superstripes.com

[1] J. Nagamatsu *et al.*, Nature (London) **410**, 63 (2001).
[2] J. H. Schön, Ch. Kloc, and B. Batlogg, Science **293**, 2432 (2001).
[3] A. Bianconi, US Patent No. 6,265,019 B1 (24 July 2001).
[4] J. Kortus, I. I. Mazin, K. D. Belashchenko, V. P. A. Tropov, and L. L. Boyer, Phys. Rev. Lett. **86**, 4656 (2001); J. M. An and W. E. Pickett, *ibid.* **86**, 4366 (2001); G. Satta, G. Profeta, F. Bernardini, A. Continenza, and S. Massidda, Phys. Rev. B **64**, 104507 (2001).
[5] A. J. Freeman, A. Continenza, M. Posternak, and S. Massidda, in *Surface Properties of Layered Structures*, edited by G. Benedeck (Kluwer, Dordrecht, 1992), and references cited therein.
[6] N. V. Vekshina, L. Ya. Markovskii, Yu. D. Kondrashev, and T. K. Voevodskyaya, Zh. Prikl. Khim. (Leningrad) **44**, 958 (1971).
[7] J. S. Slusky, N. Rogado, K. A. Regan, M. A. Hayward, P. Khalifah, T. He, K. Inumaru, S. Loureiro, M. K. Haas, H. W. Zandbergen, and R. J. Cava, Nature (London) **410**, 343 (2001).
[8] B. Lorenz, R. L. Meng, Y. Y. Xue, and C. W. Chu, Phys. Rev. B **64**, 052513 (2001).
[9] A. Bianconi, D. Di Castro, S. Agrestini, G. Campi, N. L. Saini, A. Saccone, S. De Negri, and M. Giovannini, J. Phys.: Condens. Matter **13**, 7383 (2001).
[10] A. Bianconi and A. Saccone, in *Studies of High Temperature Superconductors*, edited by A. V. Narlikar (Nova, New York, 2001), Vol. 38 ($MgB_2$), p. 153.
[11] S. Agrestini, D. Di Castro, M. Sansone, N. L. Saini, A. Saccone, S. De Negri, M. Giovannini, M. Colapietro, and A. Bianconi, J. Phys.: Condens. Matter **13**, 11 689 (2001).
[12] J. Q. Li *et al.*, cond-mat/0104320 (unpublished); J. Y. Xiang *et al.*, cond-mat/0104366 (unpublished)
[13] S. Suzuki, S. Higai, and K. Nakao, J. Phys. Soc. Jpn. **70**, 1206 (2001); J. B. Neaton and A. Perali, cond-mat/0104098 (unpublished).
[14] D. Di Castro, N. L. Saini, A. Bianconi, and A. Lanzara, Physica C **332**, 405 (2000).
[15] T. Yildirim, O. Gulseren, J. W. Lynn, C. M. Brown, T. J. Udovic, H. Z. Qing, N. Rogado, K. A. Regan, M. A. Hayward, J. S. Slusky, T. He, M. K. Haas, P. Khalifah, K. Inumaru, and R. J. Cava, Phys. Rev. Lett. **87**, 037001 (2001).
[16] W. Kohn and J. M. Luttinger, Phys. Rev. Lett. **15**, 524 (1965); H. Rietschel and L. J. Sham, Phys. Rev. B **28**, 5100 (1983); M. Grabowsky and L. J. Sham, *ibid.* **37**, 3626 (1988); Y. Takada, J. Phys. Soc. Jpn. **61**, 238 (1991).
[17] Y. J. Uemura, L. P. Le, G. M. Luke, B. J. Sternlieb, W. D. Wu, J. H. Brewer, T. M. Riseman, C. L. Seaman, M. B. Maple, M. Ishiwaka, D. G. Hinks, J. D. Jorgensen, G. Saito, and H. Yamochi, Phys. Rev. Lett. **66**, 2665 (1991); Y. J. Uemura *et al.*, Nature (London) **352**, 605 (1991); Ch. Niedermayer, C. Bernhard, U. Binninger, H. Glückler, J. L. Tallon, E. J. Ansaldo, and J. I. Budnick, Phys. Rev. Lett. **71**, 1764 (1993).
[18] F. Pistolesi and G. C. Strinati, Phys. Rev. B **49**, 6356 (1994).
[19] A. Bianconi, Solid State Commun. **91**, 1 (1994); A. Bianconi and M. Missori, *ibid.* **91**, 287 (1994); A. Bianconi, *ibid.* **89**, 933 (1994); Physica C **235–240**, 269 (1994).